

Gravitational collapse of ring objects in five-dimensional space-time

Yuta Yamada¹ and Hisa-aki Shinkai²

*Faculty of Information Science and Technology, Osaka Institute of Technology,
Hirakata, Osaka 573-0196, Japan*

Abstract

Numerical studies of gravitational collapses of ring objects are reported. We followed dynamics of collisionless particles which are distributed in toroidal configurations in non-rotating space-time, comparing their evolutions both in four and five-dimensional space-time. All the models evolve into a single spherical black-hole, while we observed a formation of ring-shaped ($S^2 \times S^1$) apparent horizon in their earlier stage for large radius ring matter in five-dimensional cases. The topology change of apparent horizon occurs as their area gradually increases. Since we do not include any rotations of space-time, all collapses proceed so quickly that no observer can be escaped from the center of the ring if he/she observed an appearance of a ring black hole.

1 Introduction

In recent years, the so-called “large extra-dimensional models” have been investigated as a consequence of brane-world pictures. It is expected that the LHC detects productions (and evaporations) of mini black-holes if our universe is constructed with higher dimension more than four. With this background, black-holes in higher dimensional space-time are extensively studied for a decade.

In such studies of higher dimensional black-hole, one of the most interesting aspects is the discovery of black-ring solution[1] with horizon of $S^2 \times S^1$ topology in $U(1) \times U(1)$ space. Discovery of black-ring solution indicates that there is no uniqueness theorem under the assumption of stationary and axisymmetry in higher dimensional space-time. Furthermore, many interesting discoveries of new black-hole solutions which are called “black objects” have been reported and their properties are being revealed.

Recently, it was suggested that fat black-ring might be unstable because of the existence of initial data which violates the local Penrose inequality[2]. However, fully relativistic dynamical features of black-ring, such as the formation processes and topological transition, are still unknown. We plan to investigate dynamical features of black-objects using numerical simulations.

In our previous work, we investigated the initial data sequences of non-rotating spheroidal and ring matter configurations[3]. We numerically solved the Hamiltonian constraint under the assumption of momentarily static and conformally flat. We found a critical ring radius for ring-shaped apparent horizon (AH) and this results indicate that a dynamical transition of horizon’s topology from toroidal to spherical may be observed in a time evolution. We also discussed the validity of the hyper-hoop conjecture using minimum area around matter. We concluded that hyper-hoop conjecture is valid for the formation of spherical (S^3) apparent horizon. Furthermore, we performed the simulation of gravitational collapses with initial data sequences of spheroidal configurations using our full general relativity code[4].

In this article, we report the gravitational collapses of non-rotating ring objects in five-dimensional space-time (5D). Our simulations does not include angular momentum, but the model would be helpful for understandings of black-ring space-time. We search both AH of spherical and ring-shaped during time evolution.

¹Email address: yamada@is.oit.ac.jp

²Email address: shinkai@is.oit.acl.jp

2 Our numerical approach

2.1 Initial data

The initial data are constructed on four-dimensional space-like hypersurface $\Sigma^{(4)}$. By assuming the time symmetry, non-trivial equation is only the Hamiltonian constraint equation. We apply the standard conformal approach to obtain the spatial metric γ_{ij} . The equations would be simplified with a conformal transformation,

$$\gamma_{ij} = \psi^2 \hat{\gamma}_{ij} \quad \text{for } \Sigma^{(4)}, \quad (1)$$

where $\hat{\gamma}_{ij}$ is a trial base metric which we assume conformal flatness as,

$$d\ell^2 = \hat{\gamma}_{ij} dx^i dx^j = dX^2 + X^2 d\theta_1^2 + dZ^2 + Z^2 d\theta_2^2, \quad \text{for } \Sigma^{(4)}. \quad (2)$$

The Hamiltonian constraint equation, then, becomes

$$\hat{D}_i \hat{D}^i \psi = -\frac{1}{3} \kappa^2 \hat{\rho} \quad \text{for } \Sigma^{(4)}. \quad (3)$$

where D_i , κ^2 and $\hat{\rho}$ express the covariant derivative, gravitational constant and total energy density, respectively. We impose the asymptotically flatness as the outer boundary condition and reflection symmetry as the inner boundary condition as following

$$\psi = 1 + \frac{M_{\text{ADM}}}{r^{N-2}} \quad (\text{at outer boundaries}), \quad (4)$$

$$\nabla \psi = 0 \quad (\text{at inner boundaries}), \quad (5)$$

where $r = \sqrt{X^2 + Z^2}$, and M_{ADM} can be interpreted as the ADM mass of the configuration.

2.2 Evolution

We developed our evolution code using the standard 4+1 ADM formalism. In the $N+1$ ADM formalism, the metric $g_{\mu\nu}$ is written as

$$g_{\mu\nu} = \begin{pmatrix} -\alpha^2 + \beta_k \beta^k & \beta_i \\ \beta_j & \gamma_{ij} \end{pmatrix}, \quad (6)$$

where μ and ν run from 0 to $N+1$ and i, j, k run from 0 to N . Evolution equations for the spatial metric γ_{ij} and the extrinsic curvature K_{ij} are written as

$$\frac{\partial \gamma_{ij}}{\partial t} = -2\alpha K_{ij} + D_i \beta_j + D_j \beta_i, \quad (7)$$

$$\begin{aligned} \frac{\partial K_{ij}}{\partial t} &= \alpha^{(N)} R_{ij} + K K_{ij} - 2\alpha K_{il} K^{lj} - \kappa^2 \alpha \left(S_{ij} + \frac{1}{N-1} \gamma_{ij} (\rho - S) \right) \\ &\quad - D_i D_j \alpha + D_i \beta^m K_{mj} + D_j \beta^m K_{mi} + \beta^m D_m K_{ij}, \end{aligned} \quad (8)$$

where α and β_i are the lapse function and shift vector, S is the trace of stress tensor, respectively. We assume the asymptotical flatness,

$$\gamma_{ij} = \delta_{ij} + \frac{\text{const}}{r^{N-2}}, \quad (9)$$

at the outer boundary. We also impose the reflection symmetry on the inner boundary.

For the lapse condition, we apply the maximal time slicing condition ($K = 0$) at $t = 0$ (for the first time step), and K-driver condition during time evolution. In 5D, the condition is given by

$$D_i D^i \alpha = \alpha \left(K_{ij} K^{ij} + 2\kappa^2 \rho - \kappa^2 S - \frac{4\kappa^2}{3} (\rho - S) \right). \quad (10)$$

We solve this elliptic equation by imposing the asymptotically flatness. Solving Eq.(10) is computationally expensive since it is an elliptic partial differential equation. During time evolution, we adopt the K-driver

condition, $\partial_t K = -cK$, (where c is a positive constant) which drives K back to zero so that the lapse function approximately satisfies the maximal time slicing condition. The K-driver for 5D is written down as

$$\frac{\partial \alpha}{\partial t} = \epsilon D_i D^i \alpha - \epsilon \alpha \left(K_{ij} K^{ij} + 2\kappa^2 \rho - \kappa^2 S - \frac{4\kappa^2}{3}(\rho - S) \right) - \epsilon \beta^i D_i K - \epsilon c K, \quad (11)$$

where ϵ acts as an effective diffusion constant. We also use zero shift condition $\beta^i = 0$ since we assume non-rotating space-time.

We use the 5D Cartoon method[5] for expressing the axisymmetric system for both the initial data set and time evolution. This method was proposed as a prescription for constructing a symmetric space-time numerically, in which the essence is not to use curvilinear coordinates but to use the Cartesian coordinates. This idea simplifies the treatment on the axis.

We express ring configurations by distributing a collisionless particles. Each particle follows the geodesic equation which we solved using the fourth-order Runge-Kutta method.

3 Numerical results

Figure 1 shows snapshots of 5D axisymmetric evolutions of ring matter which is described with 5000 particles and same ADM mass for all cases. We see that when initial ring radius is $R_c/M = 0.75$, common AH is observed at $t/M = 1.1$. While we see that when initial ring radius is $R_c/M = 1.5$, ring-shape AH is observed at $t/M = 1.7$. We also find that topological transition occur to spherical (S^3) from ring-shape ($S^2 \times S^1$) at $t/M = 2.7$.

In Fig.2, we show the area of both common and ring AHs as a function of coordinate time. We show three cases of the initial ring radius; $0.5M$, $1.5M$ and $2.0M$. Common or ring AH is formed for all cases. We see that the area of AHs monotonically increases in all cases. Furthermore, we find that the area of common AH is larger than that of ring AHs, when the topological transition is observed.

For the case of $R_c(t=0)/M = 1.5$ (right panel in Fig.1), we check whether the observer at the origin who watched the appearance of the ring AH can escape outside or not. Fig.3 shows the snapshots of the hypersurfaces on x and z axis with the proper-time. In Fig.3, solid lines colored by red, blue and green express a common and ring AH and light ray, respectively. For this case, the light ray which emitted from the inner ring AH reaches to origin at proper-time $t = 1.6$ (left panel in Fig.3). Even if the observer tries to escape with the speed of light just after that time, he/she can not move outside of the common AH.

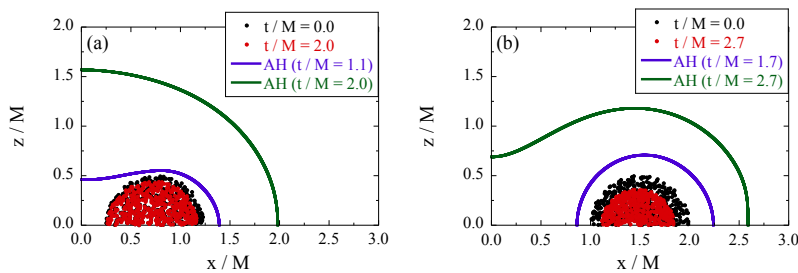


Figure 1: Snapshots of time evolutions plotting particles and location of AH. Number of particles are reduced to 1/10 for figures. We set initial ring radius to $R_c/M = 0.75$ (left panel) and $R_c/M = 1.5$ (right panel). We see that a common AH is directly formed at $t/M = 1.1$ in the left panel, while we see a topological transition of AHs to spherical from ring-shape at $t/M = 2.7$ in the right panel.

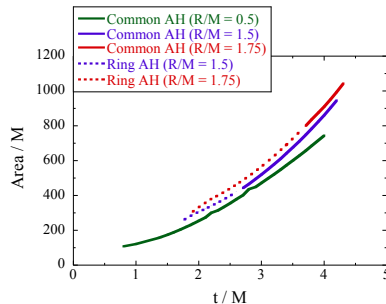


Figure 2: Area of AHs is shown for three cases that initial ring radius is $0.5M$, $1.5M$ and $2.0M$. Area is normalized with ADM mass M_{ADM} . Dotted lines express ring AH's area. Common AH's areas are expressed by solid lines. AHs monotonically increase in time. We see that the area of common AH is larger than that of the ring AHs, when the topological transition is observed.

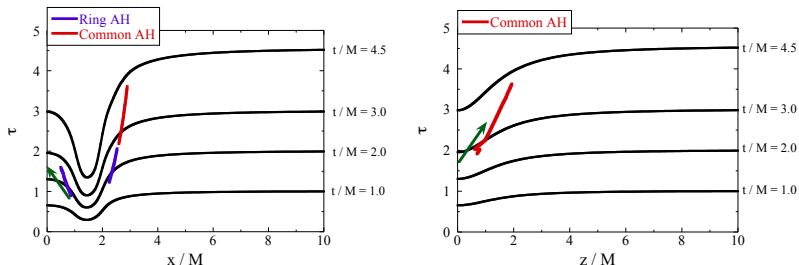


Figure 3: The snapshots of the hypersurfaces on x and z axis in the proper-time. The arrow indicates the path of light, which shows the observer at the origin cannot escape if he/she sees the appearance of a ring-shaped horizon.

4 Discussion

In this paper, we reported gravitational collapses of non-rotating ring configurations in 5D space-time. We found that topological transition of AH during the ring matter collapses where we observed monotonical increase of the area of AHs both common and ring AHs. We also found that no observer can escape from the center of the ring if he/she observed an appearance of a ring black hole since all collapses proceed so rapidly. Up to this moment, we only checked the existence of apparent horizons, and not the event horizons. The system does not include any angular momentums. We are implementing our code to cover these studies. This work was supported partially by the Grant-in-Aid for Scientific Research Fund of Japan Society of the Promotion of Science, No. 22540293. Numerical computations were carried out on SR16000 at YITP in Kyoto University, and on the RIKEN Integrated Cluster of Clusters (RICC).

References

- [1] R. Emparan and H. S. Reall, Phys. Rev. Lett. **88**, 101101 (2002).
- [2] P. Figueras, K. Murata and H. S. Reall, arXiv : 1107.5785 (2011).
- [3] Y. Yamada and H. Shinkai, Class. Quant. Grav. **27**, 045012 (2010).
- [4] Y. Yamada and H. Shinkai, Phys. Rev. D **83**, 064006 (2011).
- [5] M. Shibata and H. Yoshino, Phys. Rev. D. **80**, 084028 (2009).